

SUPPLEMENTAL MATERIALS

Figure S1, related to Figure 1.

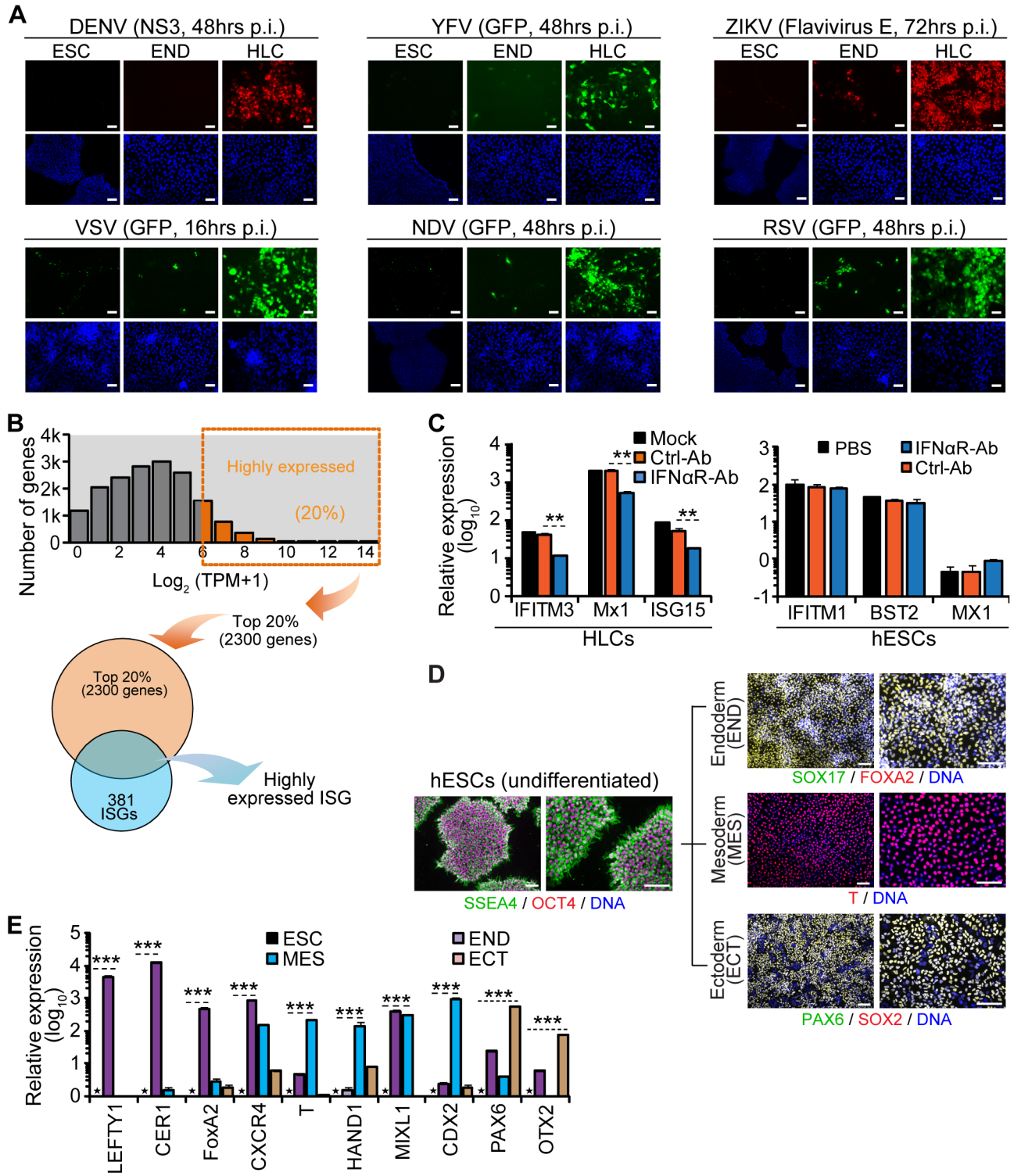


Figure S1, related to Figure 1. Intrinsic expression of ISGs in pluripotent and multipotent human stem cells

(A) Representative images showing increasing permissiveness to virus infection along hepatic differentiation of hESCs. Cells were infected with indicated viruses, fixed at the indicated time points post infection (p.i.) and were visualized directly (green, GFP-expressing viruses) or stained with the indicated antibodies (red: anti-NS3 for DENV and anti-flavivirus E for ZIKV). Nuclei were visualized by DAPI staining (lower panels in each grouping). Scale bars: 100 μ m.

(B) Schematic workflow for identifying ISG signature in stem cells. Briefly, for any given stem cell type, we focused on genes with TPM values above a minimum threshold (approximately TPM >1.0, detailed in STAR methods) in all biological replicates, thereby defined as “expressed” genes. The number of expressed genes ranged from 13,000 to 15,000, depending on the cell type and cell stage. Within the highly expressed group (top 20% of genes, ranked by TPMs), we focused on interferon-stimulated genes (ISGs), based on the compiled human and mouse ISG lists (Table S2). ISGs within the highly expressed set were defined as “highly expressed ISGs” for the cells analyzed. Shown are data from hESC line WA09.

(C) Blockade of IFN response by IFNAR2 blocking antibodies in HLCs, but not hESCs. Left: hESCs-derived HLCs were pre-treated with isotype control or IFNAR2 blocking antibodies for 4 hr, followed by stimulation with IFN- β (100U/ml) for 12 hr. The magnitude of representative ISG induction was measured by qRT-PCR. Expression in untreated HLC was utilized for normalization. Mock indicates cells not treated with antibody prior to IFN stimulation. Right: Relative expression of the indicated ISGs in hESCs after being maintained in the presence of 10 μ g/ml neutralizing antibody against IFNAR2 for 48 hr by qRT-PCR. Expression of mock cells was utilized for normalization. Shown are the means \pm SD from 3 independent experiments.

(D) Representative images at low and high magnification of hESCs and hESC-derived germ layers. Cells were stained with indicated antibodies and analyzed by IFA. Nuclei were stained with DAPI. Scale bars: 100 μ m.

(E) Relative expression of cell type-specific markers in hESCs and derived germ layers was measured by qRT-PCR. Expression levels in hESC were utilized for normalization. Shown are the means \pm SD from 3 independent experiments. Statistical analyses were calculated between ESCs and tissue stem cells, as indicated by the dotted lines.

Asterisks indicate statistically significant differences (Student’s t test was used throughout this study) (*, p<0.05; **, p<0.01; ***, p<0.001).

Figure S2, related to Figure 2.

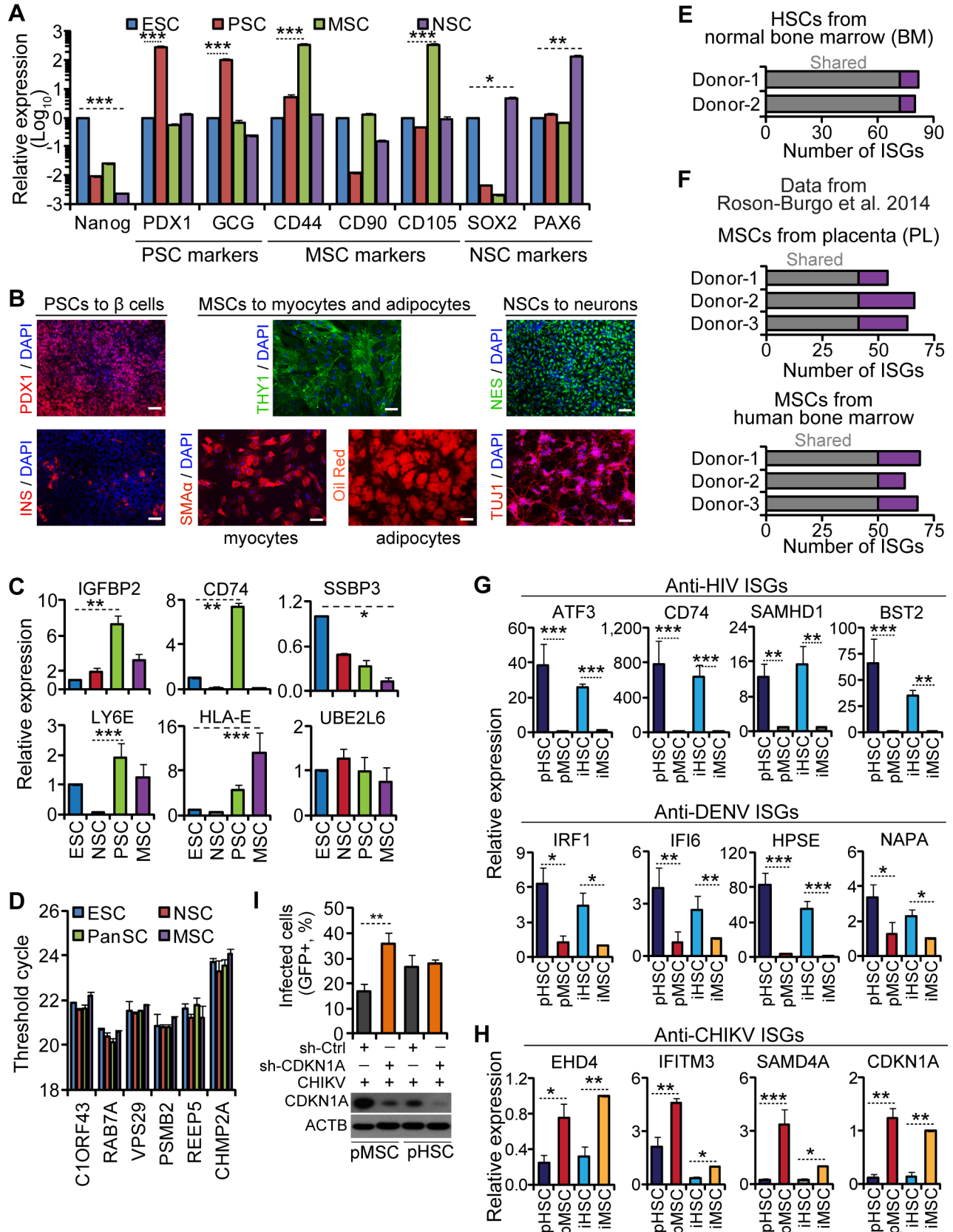


Figure S2, related to Figure 2. Distinct ISG expression patterns in different tissue stem cells

(A) Relative expression of the indicated cell type-specific markers in hESCs and derived tissue stem cells was measured by qRT-PCR. PSC makers: PDX1 and GCG; MSC markers: CD44, CD90, and CD105; NSC markers: SOX2 and PAX6. CD90 and SOX2 are also markers for hESCs. Expression levels in hESC were utilized for normalization. Shown are the means \pm SD from 3 independent experiments.

(B) Representative images showing terminal differentiation of hESC-derived tissue stem cells. The left panels represent tissue stem cells and the right panels show terminally differentiated cells. PSC to β -cell differentiation was monitored by insulin expression (INS, red); MSC to myocyte differentiation by smooth muscle actin (SMA α , red) and to adipocyte by the presence of characteristic cytoplasmic lipid droplets (oil-red staining); NSC differentiation to neuron was monitored by expression of tubulin beta 3 class III (TUJ1, red). Nuclei were stained by DAPI. Scale bars: 100 μ m

(C) Relative expression of selected ISGs in hESC and three tissue stem cells was determined by qRT-PCR. Expression levels in hESC were utilized for normalization. Shown are the means \pm SD from 3 independent experiments.

(D) Expression of housekeeping genes was measured by qRT-PCR and compared between ESCs and three tissue stem cells. Shown are the means of threshold cycles \pm SD from 3 independent experiments.

(E) Bar diagram illustrating the number of highly expressed ISGs unique to individual donor (purple) and common to both donors (gray) in HSCs isolated from bone marrow (BM).

(F) Bar diagram illustrating the number of highly expressed ISGs unique to individual donor (purple) and common to all donors (gray). Top: MSCs were isolated from placenta tissue (PL) of three donors; Bottom: MSCs were isolated from bone marrow (BM) of three donors, as described in (Roson-Burgo et al., 2014)

(G) Expression of selected ISGs (anti-HIV and anti-DENV) in primary tissue stem cells (pHSC and pMSC) and hESC-derived HSCs and MSCs (iHSC and iMSC) was measured by qRT-PCR. Primary HSCs were from fetal livers of three different donors, and MSCs were from adipose tissue of two donors; iMSCs and iHSCs were derived from hESC WA09 line. Expression levels in iMSC were utilized for normalization. Shown are the means \pm SD from 2 or 3 biological replicates and 3 independent experiments.

(H) Expression of selected ISGs (anti-CHIKV ISGs) in primary tissue stem cells (pHSC and pMSC) and hESC-derived HSCs and MSCs (iHSC and iMSC) was measured by qRT-PCR. Cells were from the same sources as described in (G). Expression levels in iMSC were utilized for normalization. Shown are the means \pm SD from 2 or 3 biological replicates and 3 independent experiments.

(I) Primary HSCs and MSCs transduced with sh-Ctrl or sh-CDKN1A were infected with CHIKV (MOI =1.0). At 16 hr p.i., the cells were harvested for analyses of CHIKV infection and CDKN1A

expression. The percentages of CHIKV infection were determined by flow cytometry for GFP (+) cells are shown (upper panel). Data are shown as the means \pm SD from 3 independent experiments. Statistically significant differences, relative to infection of sh-Ctrl are indicated. Lower panels show western blot analysis of CDKN1A. ACTB served as a loading control.

Asterisks indicate statistically significant differences (Student's t test was used) (*, $p < 0.05$; **, $p < 0.01$; ***, $p < 0.001$).

Figure S3, related to Figure 3

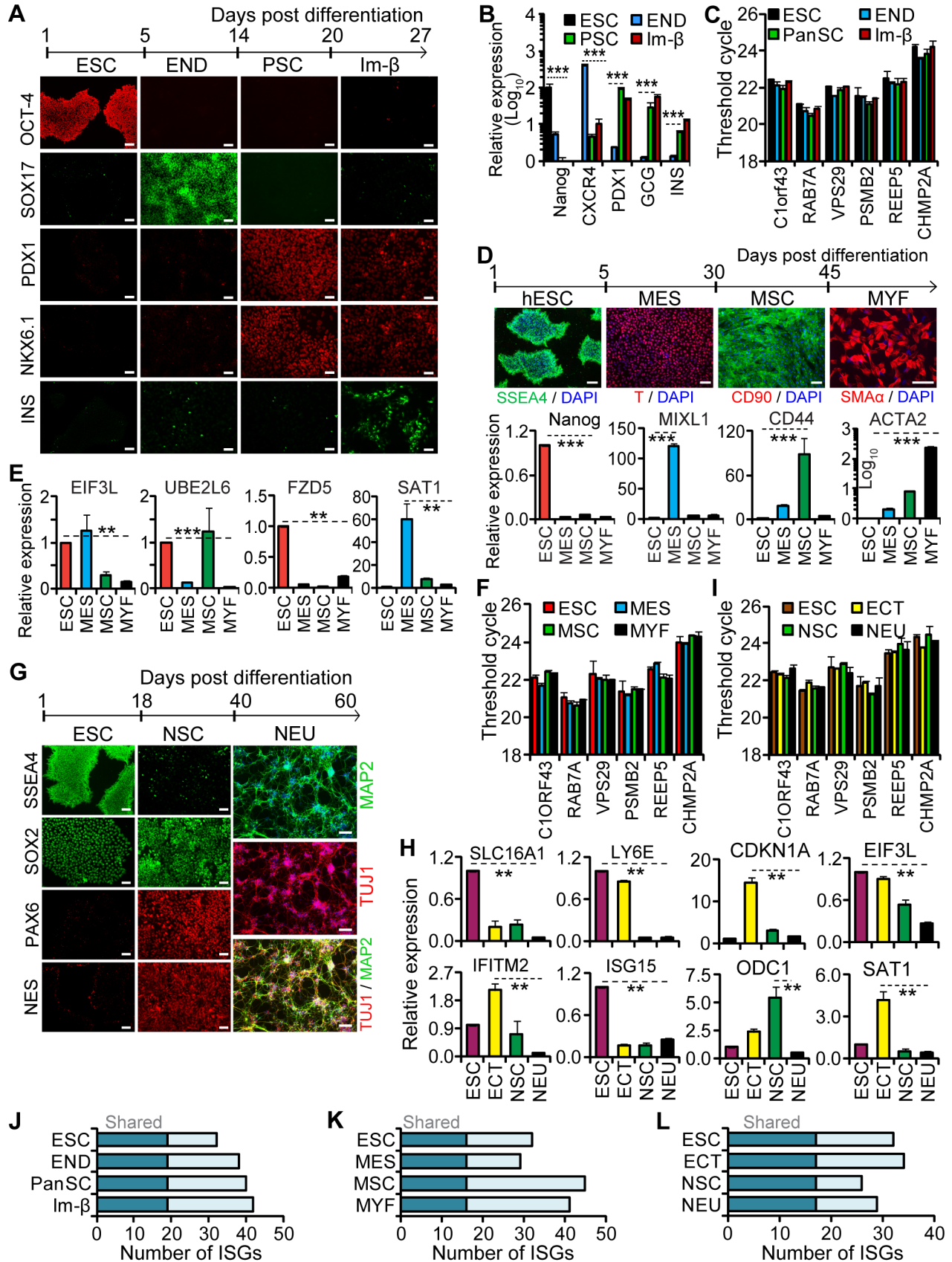


Figure S3, related to Figure 3. ISG expression changes during terminal differentiation of hESCs

(A) Pancreatic β -cell differentiation from hESCs was monitored by staining at days 0, 5, 14, 20, and 27 during the differentiation process using antibodies that recognized OCT4, SOX17, PDX1, NKX6.1, and INS, as indicated. Representative images at specified stages are shown. Scale bars: 100 μ m.

(B) Expression of the indicated stage-specific markers along β -cell differentiation from hESCs was analyzed by qRT-PCR. Shown are the means \pm SD from 3 independent experiments.

(C) Expression of the indicated housekeeping genes from cells at the specified stages along β -cell differentiation was analyzed by qRT-PCR. Shown are the means of threshold cycles \pm SD from 3 independent experiments.

(D) Top: Cells undergoing differentiation into myofibroblasts were fixed and stained with the indicated antibodies and analyzed by IFA. Nuclei were stained with DAPI and merged images are shown. Scale bars: 100 μ m.

Bottom: Expression of the indicated selected stage markers along myofibroblast differentiation was analyzed by qRT-PCR. Shown are the means \pm SD from 3 independent experiments.

(E) Expression of the indicated selected ISGs from cells at the specified stages along myofibroblast differentiation was analyzed by qRT-PCR. Shown are the means \pm SD from 3 independent experiments.

(F) Expression of the indicated housekeeping genes from cells at the specified stages along myofibroblast differentiation was analyzed by qRT-PCR. Shown are the means of threshold cycles \pm SD from 3 independent experiments.

(G) Neuronal differentiation from hESCs was monitored by staining at days 0, 18, 40, and 60 during the differentiation process using antibodies that recognized SSEA-4, SOX2, PAX6, NES, TUJ1 and MAP2, as indicated. Representative images at specified stages are shown. Scale bars: 100 μ m.

(H) Expression of the indicated selected ISGs from cells at the specified stages along neuronal differentiation was analyzed by qRT-PCR. Shown are the means \pm SD from 3 independent experiments.

(I) Expression of the indicated housekeeping genes from cells at the specified stages along neuronal differentiation was analyzed by qRT-PCR. Shown are the means of threshold cycles \pm SD from 3 independent experiments.

(J, K, L) Bar diagram illustrating the number of highly expressed ISGs unique to each stage (light blue) and shared by all lines (dark blue) along *ex vivo* differentiation of hESC into three lineages.

Asterisks indicate statistically significant differences (Student's t test was used) (*, $p < 0.05$; **, $p < 0.01$; ***, $p < 0.001$).

Figure S4, related to Figure 3.

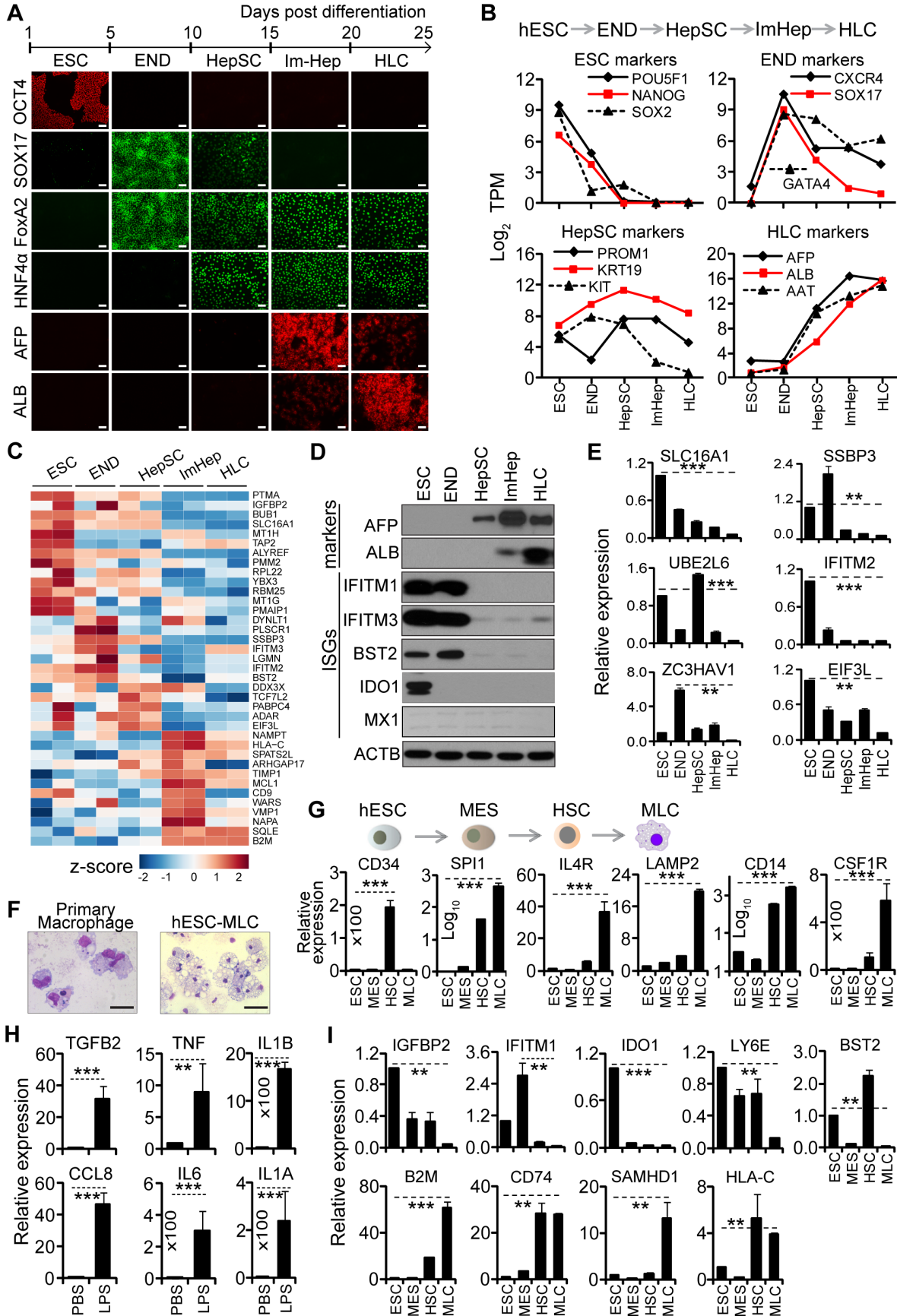


Figure S4, related to Figure 3. ISG expression changes during terminal differentiation of hESCs

(A) HLC differentiation from hESCs was monitored during the differentiation process by staining at days 0, 5, 10, 15, 20, and 25 using antibodies that recognized Oct-4, AFP and ALB followed by Alexa Fluor 594 conjugated secondary antibody (red), or SOX17, FoxA2, and HNF4 α followed by Alexa Fluor 488 conjugated secondary antibody (green). Representative images at specified stages are shown. Scale bars: 100 μ m.

(B) Relative transcript abundance of pluripotent and differentiation markers at different stages along hepatic differentiation of hESCs as measured by RNA-Seq. Data represent average log₂ TPM values for the indicated genes from two independent experiments. Five stages are shown: ESCs, END, hepatic stem cells (HepSC), immature hepatocyte (ImHep), Hepatocyte-like cells (HLC).

(C) Heatmap of RNA-Seq expression pattern (z-score TPM) of ISGs highly expressed in hESCs along *ex vivo* HLC differentiation of hESCs.

(D-E) Expression analyses of selected ISGs and markers during differentiation of hESCs along the hepatic lineage by western blot using the indicated antibodies (D) and qRT-PCR for the indicated transcripts (E). Shown in (E) are the means \pm SD from 3 independent experiments.

(F) hESC-derived macrophage-like cells (MLCs) and primary macrophage isolated from fetal liver were collected by cytopspin and stained with Giemsa. Representative images are shown. Scale bars: 100 μ m

(G) Expression of the indicated selected stage markers in cells at the specified stages during MLC differentiation is determined by qRT-PCR. Expression levels in hESC were utilized for normalization. Shown are the means \pm SD from 3 independent experiments. The morphological features of the indicated stages are shown schematically at the top.

(H) MLCs were treated for 6 hr with lipopolysaccharides (LPS, 5 μ g/ml) or PBS and RNA was isolated for qRT-PCR analysis of selected cytokines. The fold change in the LPS-treated cells relative to the PBS-treated controls for each gene is plotted. Shown are the means \pm SD from 3 independent experiments

(I) Expression of the indicated ISGs from cells at specified stages during differentiation of hESC into MLCs was measured by qRT-PCR. Expression levels in hESC were utilized for normalization. Shown are the means \pm SD from 3 independent experiments.

Asterisks indicate statistically significant differences (Student's t test was used) (*, $p < 0.05$; **, $p < 0.01$; ***, $p < 0.001$).

Figure S5, related to Figure 1.

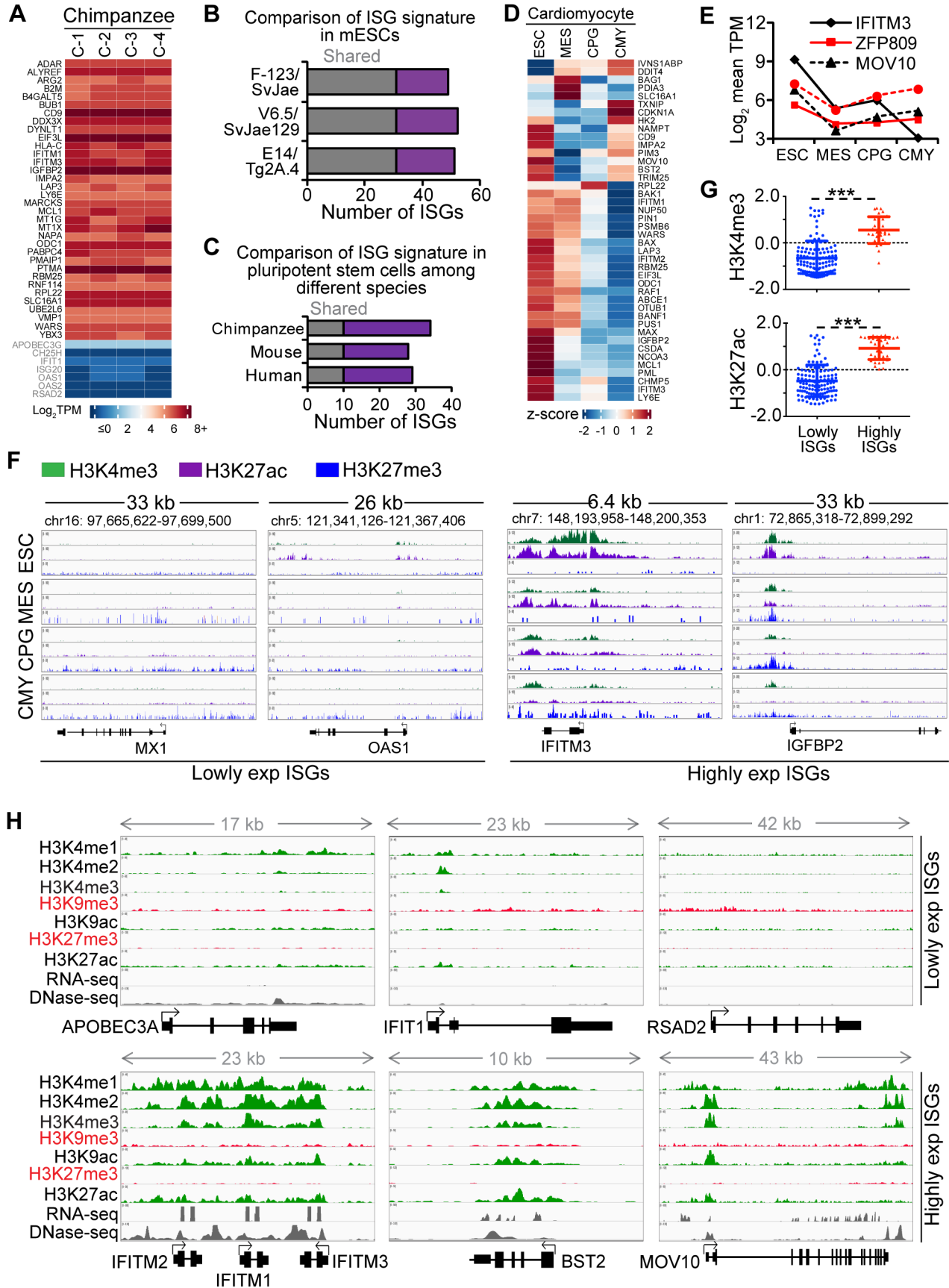


Figure S5, related to Figure 1. Intrinsic ISG expression in pluripotent and multipotent stem cells from other species

(A) Heatmap of expression patterns of highly expressed ISGs in four chimpanzee iPSC lines, \log_2 TPM. Data are from (Marchetto, et al. Nature. 2013).

(B) Bar diagram illustrating the number of highly expressed ISGs unique to each mESC line (purple) and shared by all three lines (shared/gray). Data are from (Wamstad et al., Cell. 2012; Klattenhoff et al., Cell. 2013; Li et al., PLoS One. 2014)

(C) Bar diagram illustrating the number of highly expressed pluripotent cell ISGs unique to each species (purple) or shared by all three species (shared/gray).

(D) Heatmap of gene expression (z-score TPM) for highly expressed ISGs along cardiomyocyte differentiation. Shown are highly expressed ISGs in mouse ESCs. Data are from (Wamstad et al., Cell. 2012)

(E) Relative expression of the indicated ISGs at different stages along mESCs differentiation towards cardiomyocyte. Average \log_2 TPM values of two independent experiments are shown.

(F) The epigenetic landscape showing dynamic levels of H3K4me3, H3K27ac and H3K2me3 for unexpressed or lowly expressed and highly expressed ISGs along cardiomyocyte differentiation of mESCs. Examples of lowly expressed ISGs (Lowly exp ISGs) include *MX1* and *OAS1*, and examples of highly expressed ISGs (Highly ISGs) are *IFITM3* and *IGFBP2*. ChIP-Seq (H3K4me3, H3K27ac and H3K2me3, y axis represents reads over million unique mapped reads) are shown. The scale for each modification is constant throughout the time course.

(G) Statistical analyses showing association between levels of H3K4me3 or H3K27ac and expression (RPKM) of all ISGs along cardiomyocyte differentiation of mESCs. Each dot represents value for an ISG. Shown are the means \pm SD from all the ISGs analyzed in each group. Asterisks indicate statistically significant difference (***, $p < 0.001$). For F-G, data are from published data set (Wamstad et al. 2012) and analyzed as shown in Table S4. Asterisks indicate statistically significant differences (Student's t test was used) (***, $p < 0.001$).

(H) The epigenetic landscape showing different histone modification markers, RNA-Seq, and DNase-Seq for unexpressed or lowly expressed and highly expressed ISGs in hESCs. Examples of lowly expressed ISGs (Lowly exp ISGs) include *APOBEC3A*, *IFIT1* and *RSAD2*, and examples of highly expressed ISGs (highly exp ISGs) are *IFITM1-3*, *BST2* and *MOV10*. ChIP-Seq (H3K4me1, H3K4me2, H3K4me3, H3K9me3, H3K9ac, H3K27me3, H3K27ac, y axis represents reads over million unique mapped reads) are shown. The scale for each modification is among different genes. See also Table S4 for epigenetic data.

Figure S6, related to Figure 5.

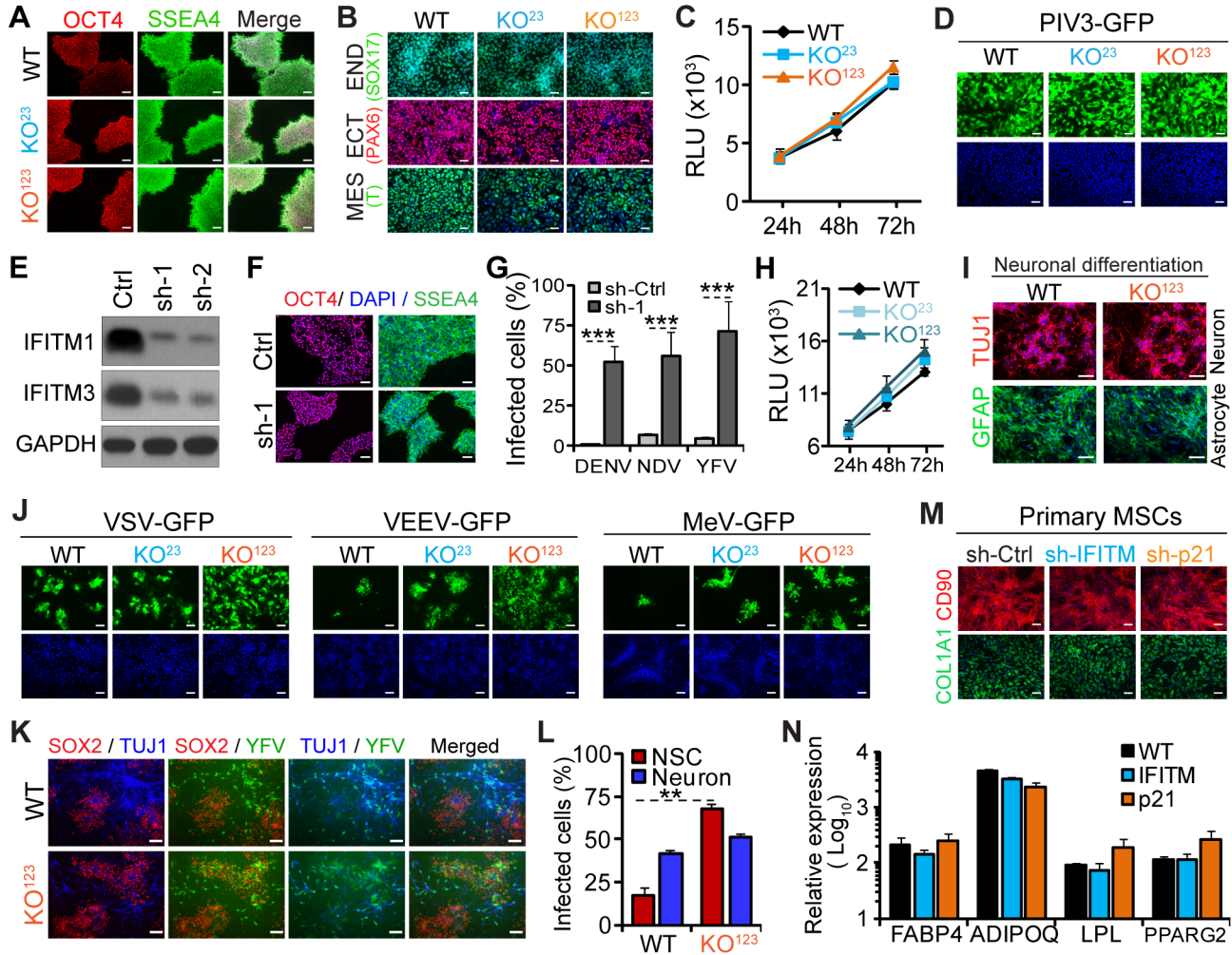


Figure S6, related to Figure 5. Antiviral activity of ISGs in human stem cells

(A) Representative images showing expression of pluripotent markers in three hESC clones. Cells were fixed and stained with the indicated antibodies. Scale bars: 100µm

(B) WT, KO²³, and KO¹²³ clones were differentiated *ex vivo* into cells representing the three germ layers and were fixed and stained with antibodies for the indicated markers. Nuclei were stained with DAPI. Representative merged images are shown. Scale bars: 100µm

(C) Equal numbers of WT, KO²³, and KO¹²³ clones were plated and at the indicated time points, viable cell numbers were determined using the CellTiter-Glo kit. Shown are the means of relative luciferase units (RLU) ± SD from 3 independent experiments.

(D) WT, KO²³, and KO¹²³ clones were infected with GFP-expressing human parainfluenza virus type-3 (hPIV3, MOI=1.0) and after 24 hr the cells were fixed and nuclei stained with DAPI. Representative images showing infection (green, top) and nuclei (blue, bottom) are shown. Scale bars: 100µm.

(E) WA09 hESCs were transduced with control (CTRL) shRNA or shRNA targeting *IFITM3* (sh-1 and sh-2) and puromycin-selected stable clones were analyzed by western blot for the indicated IFITM family members. GAPDH served as a loading control.

(F) Stable clones derived from (E) were fixed and stained with antibodies against the indicated pluripotent markers. Representative merged images are shown. Scale bars: 100 μ m

(G) Stable clones derived from (E) were infected with the indicated viruses (MOI=1.0) and after 48 hr fixed and analyzed by flow cytometry. DENV infected cells were stained with anti-NS3 antibody prior to analysis, while NDV and YFV were GFP tagged. Shown are the means \pm SD from 3 independent experiments. Asterisks indicate statistically significant differences (***, $p < 0.001$).

(H) Equal numbers of WT, KO²³, and KO¹²³ NSCs were plated and at the indicated time points, cell viable numbers were determined using the CellTiter-Glo kit. Shown are the means of RLU \pm SD from 3 independent experiments.

(I) WT and KO¹²³ NSC were differentiated into neurons or astrocytes; after fixation they were stained with antibodies against TUJ1 or GFAP, respectively. Nuclei were stained with DAPI (blue). Representative merged images are shown. Scale bars: 100 μ m.

(J) WT and KO¹²³ NSC were infected with the indicated GFP-expressing neurotropic viruses (MOI=1.0). After infection, cells were fixed and stained as follows: infections with VSV and VEEV were fixed at 12 hr p.i. and infection with MeV was fixed at 48 hr p.i. Representative images of infection (green, top) and nuclei (blue, bottom) are shown. Scale bars: 100 μ m.

(K-L) hESC-derived NSCs were cultured under conditions where NSCs gave rise to more NSCs as well as differentiated neurons; cultures were then infected with a GFP-expressing YFV (stain 17D). Cells were fixed at 48 hr p.i. and stained with NSC marker SOX2 (red) and neuronal marker TUJ1 (blue). Representative images are shown in (K). Scale bars: 100 μ m. Shown in (L) are the mean percentages of infected cells \pm SD in the NSC (SOX2⁺) and neuronal (TUJ1⁺) populations from 3 independent experiments are plotted.

(M) Primary MSCs were transduced with the indicated shRNAs [control (CTRL), *IFITM* or *p21/CDKN1A*] and 5 days later fixed and stained with the indicated antibodies against MSC markers (CD90/THY1, COL1A1). Nuclei were stained with DAPI (blue). Representative fluorescence microscopy images are shown. Scale bars: 100 μ m.

(N) Primary WT MSCs or MSCs transduced with the indicated shRNAs were differentiated into adipocyte cells and analyzed by qRT-PCR for induction of adipocyte markers. Data were normalized to RPS11 expression. Fold changes from expression levels in parental MSCs are shown as the means \pm SD from 3 independent experiments.

Asterisks indicate statistically significant differences (Student's t test was used) (**, $p < 0.01$; ***, $p < 0.001$).

Figure S7, related to Figure 7.

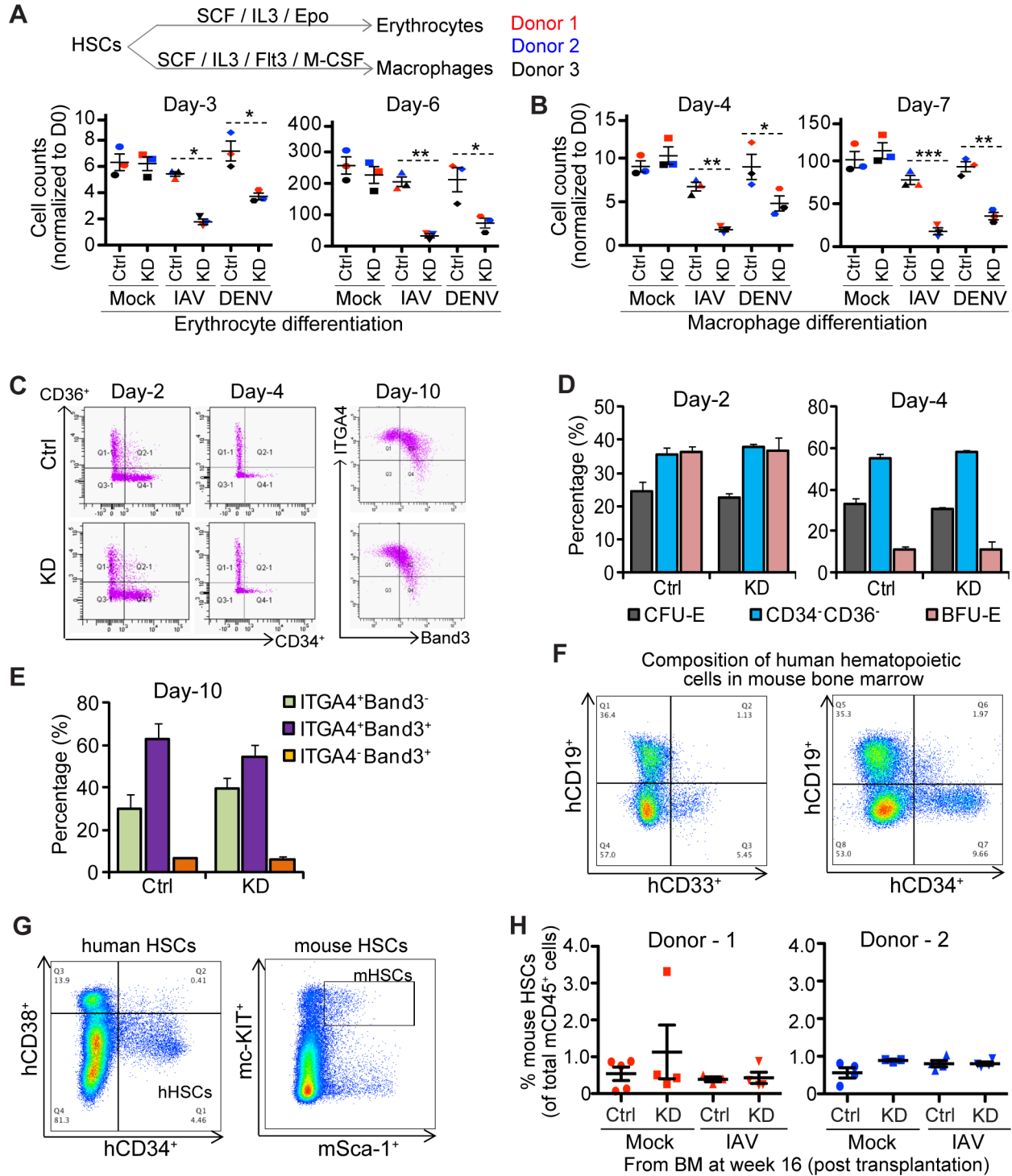


Figure S7, related to Figure 7. ISGs protect stem cells from viral infection during development.

(A-B) Top: Schematic representation of conditions for *ex vivo* differentiation of HSCs into erythrocyte and macrophage. Bottom: HSCs transduced to express control (CTRL) or IFITM shRNA (KD) were mock infected or exposed to IAV or DENV for 3 hr and then subjected to *ex vivo* differentiation into erythrocytes (A) or macrophages (B). At the indicated time points the number of

cells were counted and normalized to the number present at day 0. The means \pm SD of 3 biological replicates are shown per condition. Different colored symbols correspond to 3 different donors.

(C-E) Erythrocyte differentiation conducted in (A) was monitored at the indicated time points by flow cytometry of the indicated surface markers (CD36, CD34, ITGA4, and Band3). (C) Representative FACS plots from 3 biological replicates. (D-E) The percentages of the indicated cell types. CFU-E: colony forming unit-erythroid, defined as CD36⁺CD34⁻; BFU-E: burst-forming units-erythroid, defined as CD36⁻CD34⁺.

(F) Representative flow cytometry plots showing the composition of human leukocytes in the bone marrow from the transplanted mice described in Figure 7E-H. CD19, surface marker for human B-cells; CD33, surface marker for human cells of myeloid lineage. Shown are representative plots from mice transplanted with mock infected control HSCs. No detectable human hematopoietic cells were seen in mice transplanted with IAV pre-exposed KD HSCs.

(G) Representative flow cytometry plots showing the gating strategies for human and mouse HSCs isolated from mouse bone marrow. Human HSCs, CD34⁺CD38⁻; mouse HSCs: c-KIT⁺Sca-1⁺.

(H) Bone marrow harvested at 16 weeks from the mice described in Figure 8E-H was analyzed by flow cytometry for the percentages of murine HSCs. Each symbol represents the value obtained in an individual mouse. Bars represent the means \pm SD from n=5 mice per group from two donors.

Asterisks indicate statistically significant differences (Student's t test was used) (*, p<0.05; **, p<0.01; ***, p<0.001).